8-2015

Breast Cancer/Stromal Cells Coculture on Polyelectrolyte Films Emulates Tumor Stages and miRNA Profiles of Clinical Samples

Amita Daverey
University of Nebraska–Lincoln, amita.daverey@unmc.edu

Karleen M. Brown
University of Nebraska–Lincoln

Srivatsan Kidambi
University of Nebraska-Lincoln, skidambi2@unl.edu

Published in *Langmuir* 31 (2015), pp. 9991−10001. doi 10.1021/acs.langmuir.5b02227

Submitted June 17, 2015; revised July 30, 2015, published August 13, 2015.

Breast Cancer/Stromal Cells Coculture on Polyelectrolyte Films Emulates Tumor Stages and miRNA Profiles of Clinical Samples

Amita Daverey,[1] Karleen M. Brown,[1] and Srivatsan Kidambi[1,2,3]

1 Department of Chemical and Biomolecular Engineering, and
2 Nebraska Center for Materials and Nanoscience, University of Nebraska–Lincoln, Lincoln, NE 68588
3 Mary and Dick Holland Regenerative Medicine Program, University of Nebraska Medical Center, Omaha, NE 68198

Corresponding author — S. Kidambi, email skidambi2@unl.edu

Abstract

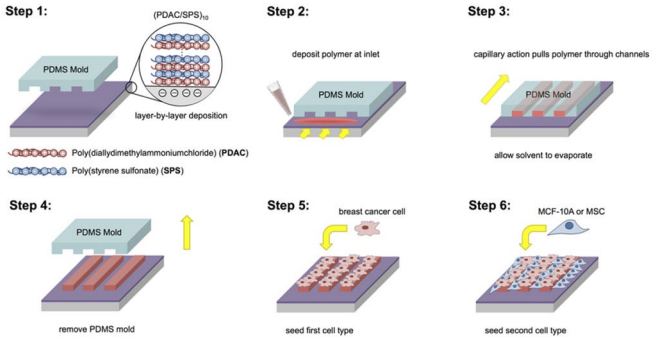

In this study, we demonstrate a method for controlling breast cancer cells adhesion on polyelectrolyte multilayer (PEM) films without the aid of adhesive proteins/ ligands to study the role of tumor and stromal cell interaction on cancer biology. Numerous studies have explored engineering coculture of tumor and stromal cells predominantly using transwell coculture of stromal cells cultured onto coverslips that were subsequently added to tumor cell cultures. However, these systems imposed an artificial boundary that precluded cell−cell interactions. To our knowledge, this is the *first demonstration* of patterned coculture of tumor cells and stromal cells that captures the temporal changes in the miRNA signature as the breast tumor develops through various stages. In our study we used synthetic polymers, namely poly(diallyldimethylammonium chloride) (PDAC) and sulfonated poly(styrene) (SPS), as the polycation and polyanion, respectively, to build PEMs. Breast cancer cells attached and spread preferentially on SPS surfaces while stromal cells attached to both SPS and PDAC surfaces. SPS patterns were formed on PEM surfaces, by either capillary force lithography (CFL) of SPS onto PDAC surfaces or vice versa, to obtain patterns of breast cancer cells and patterned cocultures of breast cancer and stromal cells. In this study, we utilized cancer cells derived from two different tumor stages and two different stromal cells to effectively model a heterogeneous tumor microenvironment and emulate various tumor stages. The coculture model mimics the proliferative index (Ki67 expression) and tumor aggressiveness (HER-2 expression) akin to those observed in clinical tumor samples. We also demonstrated that our patterned coculture model captures the temporal changes in the miRNA-21 and miRNA-34 signature as the breast tumor develops through various stages. The engineered coculture platform lays groundwork toward precision medicine wherein patient-derived tumor cells can be incorporated within our in vitro models to identify potential pathways and drug treatment regimens for individual patients.

1. Introduction

Breast cancer is one of the leading causes of death worldwide and is forecasted to increase by over 50% from 283 000 in 2011 to 441 000 in 2030 in the United States.[1] Recent studies have demonstrated that tumor microenvironment (TME) plays an important role in neoplastic transformation, tumor growth and invasion, and therapeutic resistance.[2−4] TME components composed of stromal cells such as fibroblasts, mesenchymal stem cells (MSCs), and immune cells provides a supportive niche that promotes the growth and invasion of tumors and is believed to modulate drug responsiveness.[5−7] The intercellular communication between tumor cells and stromal cells occurs via direct contact and paracrine signaling through the recruitment of growth factors, cytokines, and chemokines.[8−10] Together, these modes of communication are believed to mediate tumor expansion, invasion, metastasis, and angiogenesis. Several studies demonstrate direct involvement of stromal cells like fibroblasts, normal epithelial cells, and MSCs in progression of tumorigenesis and metastasis.[5−7] However, the exact role of different stromal cells in the TME, their interaction with each other and with the cancer cell in the progression of tumor has not been fully delineated. *Despite the importance of this cell−cell communication, the current scientific understanding remains limited on the interaction between the tumor cells and the surrounding cells due to the lack of appropriate tumor models*.

In vivo models have been primarily used to study the involvement of tumor−TME interactions in cancer.[11−14] However, these models are proving to be insufficient, as they do not lend themselves as readily to rigorous mechanistic manipulations and quantitative analysis to maximize the information that can be obtained regarding the dynamics of cell−cell interactions. Xeno-

graft animal models of human tumors are widely used as in vivo models for studying cancer metastasis and drug screening.[15,16] However, these models do not accurately recreate the various components of TME and do not allow direct observation of the tumor during the course of the treatment. There is an increasing interest in the development of in vitro tumor models due to the ease of manipulation and shorter time frame compared to an in vivo model.[17−20] However, given the complexity of breast tumor, the challenge of designing an effective in vitro model is huge. Tumor tissues, the commonly used in vitro model, lack many characteristics of intact tumor, such as TME and metabolic demand. Although great effort has been put into developing in vitro human tumor models as well as 2D and 3D gel culture systems to model TME, significant hurdles remain.[19−21] *One major limitation of the current models is that they fail to combine different types of cells, or establish cocultures of tumor cells with stromal cells in vitro*. Random and transwell cocultures are commonly used to study the role of cell−cell interactions in cancer invasion.[22,23] These approaches are limited by poor reproducibility leading to inconsistent results. They also do not account for the physical contact between the cells that is established when the tumor cells recruit the stromal cells. Therefore, alternative in vitro platforms are necessary to study the interaction of cancer cells with stromal cells.

Recently, in vitro coculture models have been fabricated on nano/micropatterned surfaces using a variety of microfabrication techniques, ranging from photolithography, microcontact printing, dip-pen spotting, to inkjet printing.[22,24−27] These resulting in vitro patterned coculture models serve as a platform for studying cell−cell communication in a controlled environment of spatially defined nano/microscale surface. This addresses the limitations associated with random coculture and transwell coculture methods by not only providing a robust and reproducible means of recreating cell−cell interactions but also accounting for both direct and paracrine modes of communication. Most of these microfabrication methods rely on approaches that utilize adhesive proteins for cell attachment and a background surface that resist that are modified later for the attachment of a second cell type.[26−28] Although these techniques allow for recreating the cellular microenvironment, the use of protein substrates adds an artificial component not present in the TME and does not mimic physiologically relevant interactions. The current in vitro method is limited due to the requirement of specialized materials, devices, and extensive expertise.

Herein, we report a robust, inexpensive, protein free method that utilizes polyelectrolyte multilayers (PEMs) and capillary force lithography (CFL) to generate patterned coculture models of breast cancer cells and stromal cells. PEMs have been shown to be excellent candidates for biomaterial applications.[28−38] In our study, we used synthetic polymers, namely, poly(diallyldimethylammonium chloride) (PDAC) and sulfonated poly(styrene) (SPS), as the polycation and polyanion, respectively, to build the multilayers. The choice of SPS and PDAC was based on previous studies, wherein the latter material was shown to be resistant to attachment by primary hepatocytes,[39] smooth muscle cells,[40] and primary neuronal cells,[41] while SPS was cytophilic for all the cell types evaluated. We as well others have previously shown that PEM surfaces utilizing PDAC and SPS also provide an ability to control the arrangement of multiple cell types with subcellular resolution.[24,25,35,39] This technique allows the formation of cell patterns with different shapes and sizes of tunable directional properties, recreating cell−cell interactions in a highly controlled manner. In addition, since CFL is a variant of soft lithography, this method has key advantages, such as low cost, high-throughput, and the ability to pattern reproducible macroscopic areas. In this study, we capitalized upon the differential cell attachment and spreading of breast cancer cells on different PEM surfaces to engineer patterned cocultures of breast cancer cells and stromal cells. To demonstrate the translational validity of our platform, we employed two developmentally distinct human breast cell lines for coculture development: (1) BT474 (HER2+ invasive breast cancer cells to model invasive ductal carcinoma (IDC)) and (2) 21MT-1 (stable patient-derived metastatic breast cancer cells isolated from the metastatic pleural effusion to model invasive mammary carcinoma (IMC)). We also used two different types of stromal cells, mammary epithelial cells (MCF10A) and mesenchymal stem cells (MSCs), to demonstrate the versatility of our platform. Since MCF10A are nontumorigenic cells and MSCs have a significant role in metastasis, our platform provides an opportunity to study cell−cell interactions in a heterogeneous TME, an inimitable property of cancer progression. We further illustrated that our in vitro breast tumor model is capable of staging the breast tumor dynamics and emulating clinical relevant molecular pathways at different stages of tumor points. For this purpose, we utilized the coculture system developed in this study and demonstrated that our platform simulated key clinical markers prominently used for tumor diagnosis, including tumor (HER-2) and proliferation (Ki67) markers. Also our platform mirrored the clinical conditions when probed for miRNA-21 and miRNA-34 expression. The development of such in vitro models that recapitulates the in vivo like signaling in tumor would be desirable to increase the drive toward precision medicine to identify key biomarkers for early diagnosis and novel therapeutic interventions.

2. Materials And Methods

2.1. Materials. Poly(diallyldimethylammonium chloride) (PDAC) (MW ~ 100,000−200,000) as a 20 wt % solution, sulfonated poly(styrene) sodium salt (SPS) (MW ~ 70 000), sodium chloride, bovine serum albumin (BSA), PKH26 cell staining kit, carboxyfluorescein succinimidyl ester (CFSE), carboxyfluorescein diacetate succinimidyl ester fluorescent dyes (CFDSE), alpha-Minimum Essential Medium (α-MEM), sodium bicarbonate ($NaHCO_3$), and cholera toxin were purchased from Sigma-Aldrich Corporation (St. Louis, MO). Poly(dimethylsiloxane) (PDMS) from the Sylgard 184 silicone elastomer kit (Dow Corning, Midland, MI) was used for making stamps. DMEM/F12 medium, fetal bovine serum (FBS), horse serum, penicillin−streptomycin, L-glutamine, 4-(2-hydroxyethyl)-1-piperazineethanesulfonic acid (HEPES), nonessential amino acids, and sodium pyruvate were purchased from Life Technologies (Gaithersburg, MD).

2.2. Cell Lines and Culture Conditions. Adipose-derived MSCs and MCF10A cells were purchased from American Type Culture Collection (ATCC). MSCs were maintained in MSCGM (Lonza) supplemented with growth factors provided with the kit, and MCF10A cells were maintained in phenol red free DMEM/F12 culture medium supplemented with $NaHCO_3$ (1200 mg/L), 5% horse serum, insulin (10 μg/mL), penicillin G (100 U/mL), streptomycin (100 μg/mL), L-glutamine (2 mM), EGF (20 ng/mL), hydrocortisone (500 ng/mL), and cholera toxin (100 ng/mL). HER-2 overexpressed breast cancer cell lines, BT-474 and 21MT-1, were a kind gift from Dr. Hamid Band (UNMC, Omaha, NE). BT-474 cells were grown in complete MEM supplemented with 5% FBS, 1% L-glutamine, penicillin G (100 U/mL), streptomycin (100 μg/mL), 20 mM HEPES, nonessential amino acids, and sodium pyruvate (complete α-MEM). 21MT-1 cells

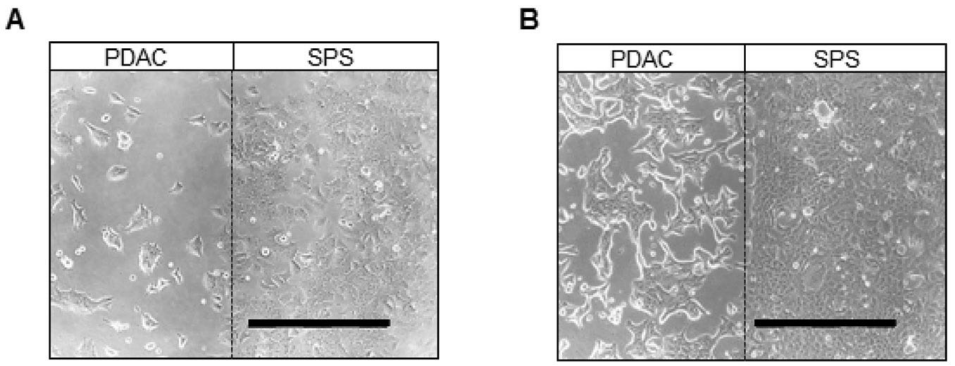

Figure 1. Breast cancer cells on polyelectrolyte multilayers. Selective adhesion of breast cancer cells on fabricated surfaces was determined by studying the growth of cells on PEMs for 5 days. Half TCPS was coated with $(PDAC/SPS)_{10}$ and other half with $(PDAC/SPS)_{10.5}$ making SPS and PDAC as the topmost surfaces, respectively. Adhesion of BT-474 (A) and 21MT-1 (B) cells on PDAC and SPS surfaces after day 5 of culture show more attachment of cells on SPS surface. Scale bar is 500 μm.

were maintained in complete α-MEM, further supplemented with EGF (12.5 ng/mL) and hydrocortisone (1 ng/mL). All cells were maintained in the presence of 5% CO^2 at 37 °C.

2.3. Cell Adhesion on Polymer Surfaces. Polyelectrolyte multilayers (PEMs) were built on tissue culture polystyrene surface (TCPS) using layer-by-layer assembly of PDAC and SPS polymers as described earlier.[24,25] The concentrations of the PDAC and SPS solutions were 0.02 and 0.01 M, respectively, using repeating unit molecular weight. Both polymers were dissolved in deionized (DI) water with 0.1 M concentration of sodium chloride followed by filtration through filter paper (pore size < 25 μm). TCPS were treated with oxygen plasma for 5 min using a Harrick plasma cleaner (Harrick Scientific Corporation, Broading Ossining, NY). The plate was immediately inserted into a Carl Zeiss slide stainer to carry out the automated layer-by-layer assembly process. Briefly, the plate was first dipped into the PDAC solution for 20 min followed by two 5 min washing steps in DI water with agitation. The plate was then dipped in the SPS solution for 20 min followed by two 5 min washing steps in DI water with agitation. This process was repeated for either 10 or 10.5 bilayers to form $(PDAC/SPS)_{10}$ with SPS as a topmost layer and $(PDAC/SPS)_{10.5}$ with PDAC as a topmost layer. Prior to cell culture, fabricated surfaces were sterilized overnight under UV. Breast cancer cells were grown on SPS [$(PDAC/SPS)_{10}$], PDAC [$(PDAC/SPS)_{10.5}$] for 5 days. Cell morphology was assessed by optical microscopic images of the cells on different surfaces acquired with Axiovert40 Zeiss (Germany) inverted microscope for 5 days.

2.4. Polydimethylsiloxane (PDMS) Mold Fabrication. PDMS molds were fabricated by combining the PDMS prepolymer (Sylgard 184, Essex Chemical) and curing agent in an 8:1 w/w ratio. Following vigorous mixing, the mixture was degassed in a desiccator until bubbles were no longer visible and cast against a silicon master that contained a pattern of line channels. The PDMS was cured for 8 h in a 60 °C oven. After cooling to room temperature, a sharp scalpel and tweezers were used to remove the PDMS from the master and cut into stamps capable of fitting within a well of a six-well plate (approximately 5 mm by 5 mm). Stamps were cleaned with ultrapure 18 MΩ cm Millipore water and soap, and then dried with compressed air before use.

2.5. Fabrication of Patterned Surfaces by Capillary Force Lithography (CFL). Line patterns were created on PEMs built on TCPS surfaces using CFL. Patterned PDMS molds (discussed previously) were activated with oxygen plasma for 1 min and placed pattern-down on the PEM-coated substrate. Slight pressure was applied to the mold to ensure good contact. Ten μL of the polymer solution that possesses a charge opposite to the last layer of the PEM was injected into the channel openings (i.e., PDAC for [$(PDAC/ SPS)_{10}$] or SPS for [$(PDAC/SPS)_{10.5}$]). The solution was drawn through the channels by capillary action, and the mold was undisturbed until solvent evaporation was completed. Once finished, the PDMS was carefully removed along the channel patterns. The surface was rinsed with DI water to remove excess polymer and dried at room temperature. To generate more complex grid patterns for potential tricultures, CFL was repeated on the patterned substrate, positioning the PDMS mold at a 90-degree rotation.

2.6. Characterization of Patterns. Generated patterns were visualized using 6-carboxyfluorecein succinimidyl ester (CFSE), rhodamine B, and negatively charged carboxylated polystyrene microparticles. Fabricated surfaces were incubated with CFSE or rhodamine B or microparticles for 10 min at room temperature, followed by three washes with DI water. Fluorescent and phase contrast images of patterns were observed and captured using Axiovert40 Zeiss inverted microscope (Germany).

2.7. Cell Staining and Coculture. For visualization of cell patterns, breast cancer cells and stromal cells were prestained prior to seeding on patterned substrates. Two different cell types were distinguished from one another by staining with carboxyfluorescein diacetate succinimidyl ester (CFDSE) dye (green) and PHK26 dye (red), respectively. Briefly, cells were trypsinized and washed with medium without serum. Cells were subsequently incubated in 10 μg/ mL CFDSE in PBS solution at a concentration of 1×10^7 cells/mL or in 2×10^6 M PKH26 in diluent C at a concentration of 1×10^7 cells/ mL for 10 min at room temperature. Both staining reactions were quenched with the addition of an equal volume of serum and washed three times with medium. After a final wash, the cell pellet was suspended in medium, and 0.5×10^6 breast cancer cells were seeded. On the following day, 0.2×10^6 MSCs or MCF10As were seeded. Fluorescent images of the cells patterns were acquired with Axiovert40 Zeiss (Germany) inverted microscope before and after coculture.

2.8. Western Blotting. Cells were washed three times with ice cold-phosphate buffered saline (PBS) and scraped in RIPA buffer (100 mM Tris, 5 mM EDTA, 5% NP40, pH-8.0) containing protease inhibitors cocktail (PIC) and phenylmethylsulfonyl fluoride (PMSF) followed by 10 min incubation on ice with intermittent vortexing. Clear cell lysate from all coculture systems was obtained by centrifugation at 10 000 rpm for 10 min at 4 °C and stored at −80 °C until use. Protein concentration was determined using Coomassie Plus Assay reagent purchased from Pierce (Rockford, IL). An am amount of 10 μg of total protein was separated by 7.5% SDS-polyacrylamide gel electrophoresis and transferred to Immobilon P membranes (Millipore, Ballerica, MA) using transfer buffer (25 mM Tris, 192 mM glycine, 10% methanol). Membranes were blocked with 5% skimmed milk for 3 h at room temperature (RT) thereafter membranes were incubated with primary antibodies for overnight at 4 °C. Anti-HER-2 (1:1000), anti-Ki67 (1:1000), or anti-GAPDH (1:4000) primary antibodies were used followed by incubation with corresponding horse peroxidase-conjugated secondary antibodies (1:5000) at room temperature (RT) for 1 h. Signal was detected using ECL and exposure to ECL Hyperfilm (Pierce, Rockford, IL). Densitometry was performed using Image Studio Lite Software ver 4.0 (LI-COR Biosciences).

2.9. miRNA Isolation and qRT-PCR. Total miRNAs were isolated from cells using the miRNeasy isolation mini-kit (Qiagen). Quality and quantity of isolated miRNAs were tested using a ND-1000 spectropho-

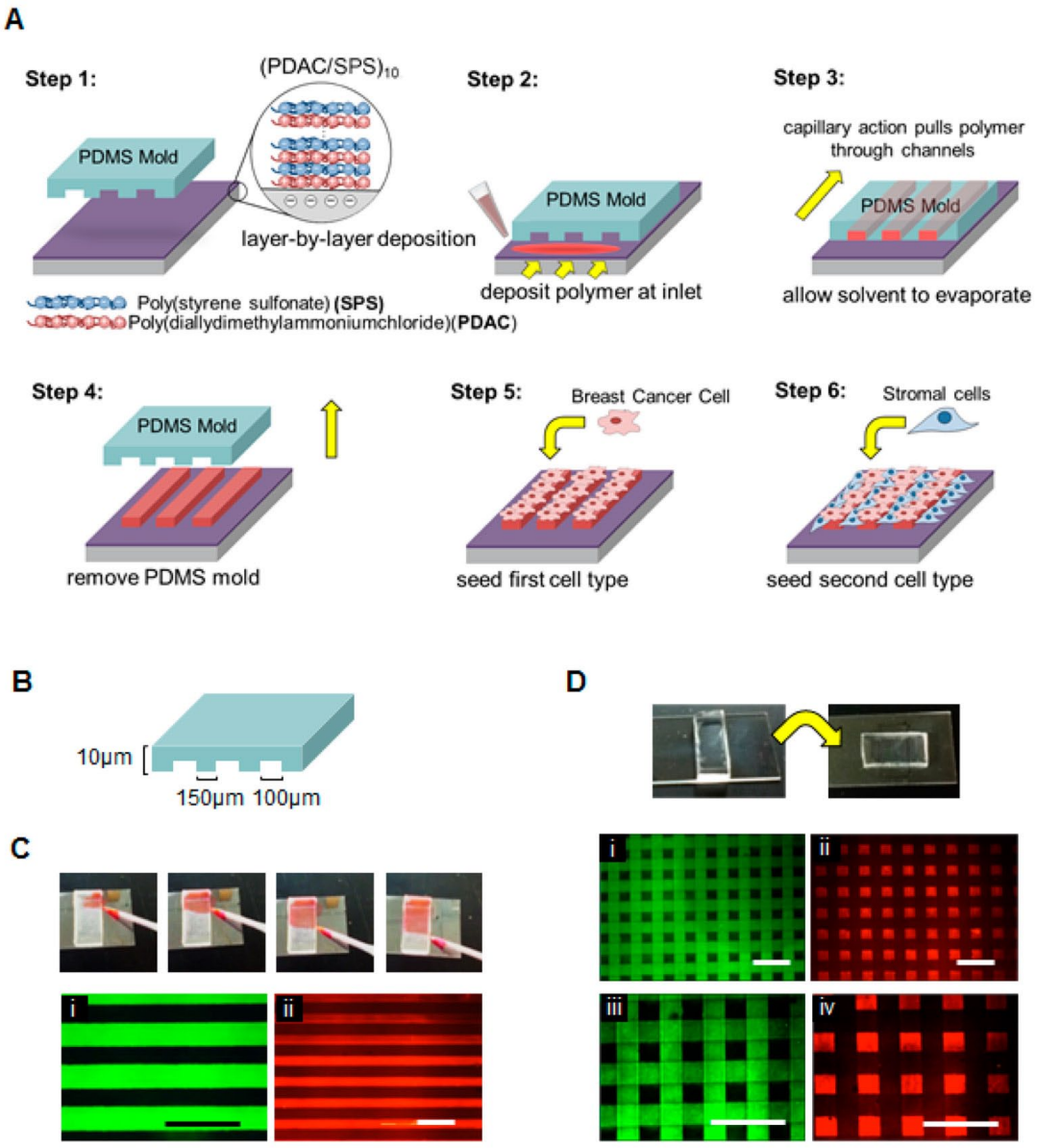

Figure 2. Characterization of patterns.

(**A**) Schematic overview for employing PEMs and CFL to create patterned coculture platform of breast cancer cells and stromal cells. First, 10.5 bilayers of PDAC and SPS were deposited to a substrate using layer-by-layer deposition to generate PDAC as a topmost layer. SPS polymer was deposited through channels of PDMS stamp using capillary force to generate polymer patterns. Breast cancer cells were seeded on patterned surfaces followed by seeding of stromal cells on day 3 to generate patterned coculture.

(**B**) Dimensions of PDMS mold employed.

(**C**) Characterization of polymer patterns generated using CFL. Patterns were characterized using green dye CFSE (i); red dye rhodamine B (ii). Scale bar is 200 μm.

(**D**) Complex grid patterns visualized with CFSE (i, iii) and rhodamine B (ii, iv). Scale bar is 500 μm.

tometer (NanoDrop Technologies, Wilmington, DE). The Mir-X miRNA First-Strand Synthesis Kit (Clontech) was used for converting miRNAs into cDNA to enable specific miRNAs to be quantified by real-time PCR. The SYBR Advantage qPCR Premix (Clontech) and mRQ 3′ (Clontech) primer were then used in real-time qPCR, along with miRNA-specific 5′ primers, to quantify miR-21 and miR-34a in the cDNA. Sequences for miR-21 and miR-34a 5′ primers were: 5′-TAGCTTATCAGACTGATGTTGA-3′ and 5′-TGGCAGTGTCTTAGCTGGTTGT-3′ respectively. Quantitative PCR for miR-21 and miR-34a was performed in epgradient S Mastercycler (Eppendorf) using a program: denaturation at 95 °C for 10 s, followed by 45 cycles of 95 °C for 5 s and 60 °C for 20 s. At the end, one cycle for dissociation curve was performed at 95 °C for 60 s, followed by 55 °C for 30 s and 95 °C for 30 s. Data were analyzed using comparative delta−delta Ct method described earlier for which an additional qPCR was performed using U6 snRNA controls provided in SYBR Advantage qPCR Premix kit.[42]

3. Results

3.1. Breast Cancer Cells on Polyelectrolyte Multilayers. To investigate the effects of PEM films on breast cancer cells, we assessed the response of breast cancer cells over continuous culture (Figure 1). For this purpose we utilized poly(diallyldimethylammonium chloride) (PDAC) and poly(4- styrenesulfonic acid) (SPS) as the polycation and polyanion, respectively, to build the PEM films. PDAC and SPS are strong polyelectrolytes, resulting in smooth, homogeneous and stable PEM films suitable for cellular studies.[43−45] The combination of PDAC and SPS has been widely employed to construct PEMs, although less work on cell adhesion has been done on this pair of polyelectrolytes than on other pairs such as poly(acrylic acid)/polyallylamine, PAA/PAH, or the more biomolecular poly(glutamic acid)/polylysine, PGA/PLL. The choice of PDAC was based on our previous studies, wherein this material was shown to be cell-resistant for primary hepatocytes, neurons, and breast cancer cells.[24,25,42] Recent study has demonstrated that PEMs using PDAC and SPS resulted in quasi-spherical cell clusters and attributed this differential cell adhesion due to the presentation of surface charges in different conditions.[35] The thin films used for the cell studies

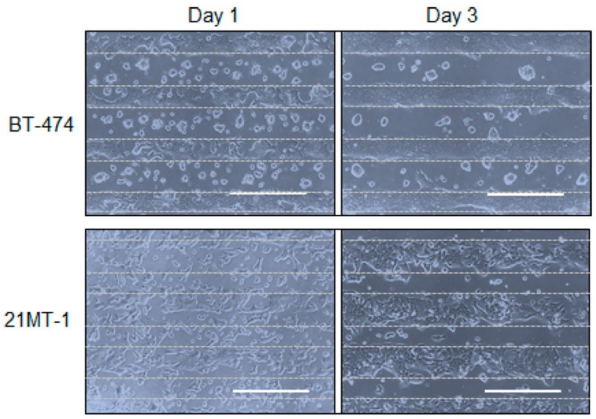

Figure 3. Patterned culture of breast cancer cells on PEMs. Breast cancer cells patterns on day 1 and day 3 of cultures. On day 3 of culture, breast cancer cells form clear patterns distinct from surround background. Scale bar is 500 μm.

were free of adhesive proteins or ligands. We employed two developmentally distinct human breast cell lines for coculture development: (1) BT474 (HER2+ invasive breast cancer cells) and (2) 21MT-1 (stable patient-derived metastatic breast cancer cells isolated from the metastatic pleural effusion). We have previously shown that breast cancer cells, BT-474 and SKBr3 cells, attached more on SPS surfaces than PDAC.[42] Figure 1 compares the morphology of breast cancer cells on PDAC and SPS surfaces. For the direct comparison of the cell adhesion, we coated half the TCPS with $(PDAC/SPS)^{10}$ and other half with $(PDAC/SPS)^{10.5}$ making SPS and PDAC as the topmost surfaces, respectively. Both BT-474 and 21MT-1 had higher attachment on SPS surfaces compared to PDAC surfaces demonstrating the preferential attachment of breast cancer cells on SPS over PDAC. We utilized this differential cell adhesion to develop patterned coculture of breast cancer cells with stromal cells.

3.2. Patterned Culture of Breast Cancer Cells on PEMs. Figure 2A shows a schematic diagram of overall strategy we used to develop patterned coculture. For patterning with CFL, thin layers of polymers were deposited using layer-by-layer assembly and a liquid prepolymer of PDMS was cast against a silicon master to prepare a PDMS mold. PDMS is excellent material for mold preparation because of its high permeability for air to permeate out of the mold during molding process, an important characteristic for high resolution patterning. In addition, PDMS chemical inertness, low surface tension, favorable mechanical and optical properties, and simple manufacturing make it compatible with CFL methods, yielding robust microstructures over substrates regardless of patterning materials. Since CFL relies on naturally occurring capillary force without use of any external force, it offers a number of advantages in fabricating geometry-controllable, robust micro and nanostructures over a large area. Dimensions of patterns used for this study are shown in Figure 2B. Patterning of polymer occurs when a liquid wets capillary tubes and moves forward with lowering of free energy (Figure 2C). Fabricated patterns were then characterized with fluorescent dyes (negatively charged CFSE and positively charged rhodamine), and negatively charged microparticles. The charges of the dye and microparticles mediate the ionic interaction on the surface, with the negatively charged macromolecules

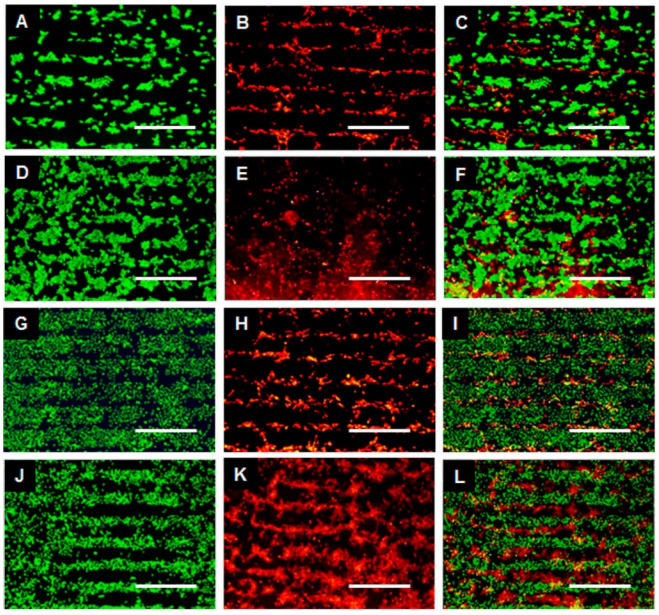

Figure 4. Patterned cocultures of tumor cells with stromal cells. BT- 474 and 21MT-1 breast cancer cells were stained with green dye CFDSE prior to seeding cells on patterns. Stromal cells, MSCs and MCF10A, were stained with red dye, PKH26 dye. Left panel shows monochrome fluorescent images of BT-474 cells (**A**, **D**) and 21MT-1 cells (**G**, **J**). Middle panel shows monochrome fluorescent images of MSCs (**B**, **H**) and MCF10A (**E**, **K**). Right panel represents merged image of BT-474/MSCs (**C**); BT-474/MCF10A (**F**); 21MT-1/MSCs (**I**); 21MT-1/MCF10A (**L**). Scale bar is 500 μm.

deposited on PDAC surfaces while the positively charged macromolecules deposited on SPS surfaces. Our data illustrated that the SPS/PDAC micropatterns were successfully created on glass substrates with good coverage and well-defined edges (Figure 2C). To further demonstrate the ability to recreate more complex microenvironment for cell−cell interaction, we fabricated intricate patterns by repeating CFL, positioning the PDMS mold at a 90-degree rotation. The stained patterns with CFSE and rhodamine shows formation of complex patterns indicating the PDAC and SPS regions (Figure 2D).

Figure 3 illustrates the attachment of breast cancer cells on PDAC and SPS patterns after one and 3 days of culture. When presented with the patterned surface, both BT-474 and 21- MT1 adhered preferentially on the SPS regions resulting in patterns of breast cancer cells. On day 1, breast cancer cells attached preferentially on the SPS regions resulting in cell patterns. The breast cancer patterns attached and maintained their morphology for the first few days, but by day 7 began to detach from the PEM surfaces due to overcrowding (data not shown). We further optimized the media composition and identified 1:1 ratio of breast cancer cells and MSCs or MCF10A media as the best culture conditions for the coculture platform (Supporting Information Figure 1).

3.3. Patterned Cocultures of Tumor Cells with Stromal Cells. Figure 4 illustrates patterned cocultures of breast cancer cells with stromal cells on PEM surfaces. We employed two developmentally distinct human breast cell lines for coculture development: (1) BT474 (HER2+ invasive breast cancer cells to model IDC) and (2) 21MT-1 (stable patient-derived metastatic breast cancer cells isolated from the metastatic pleural effu-

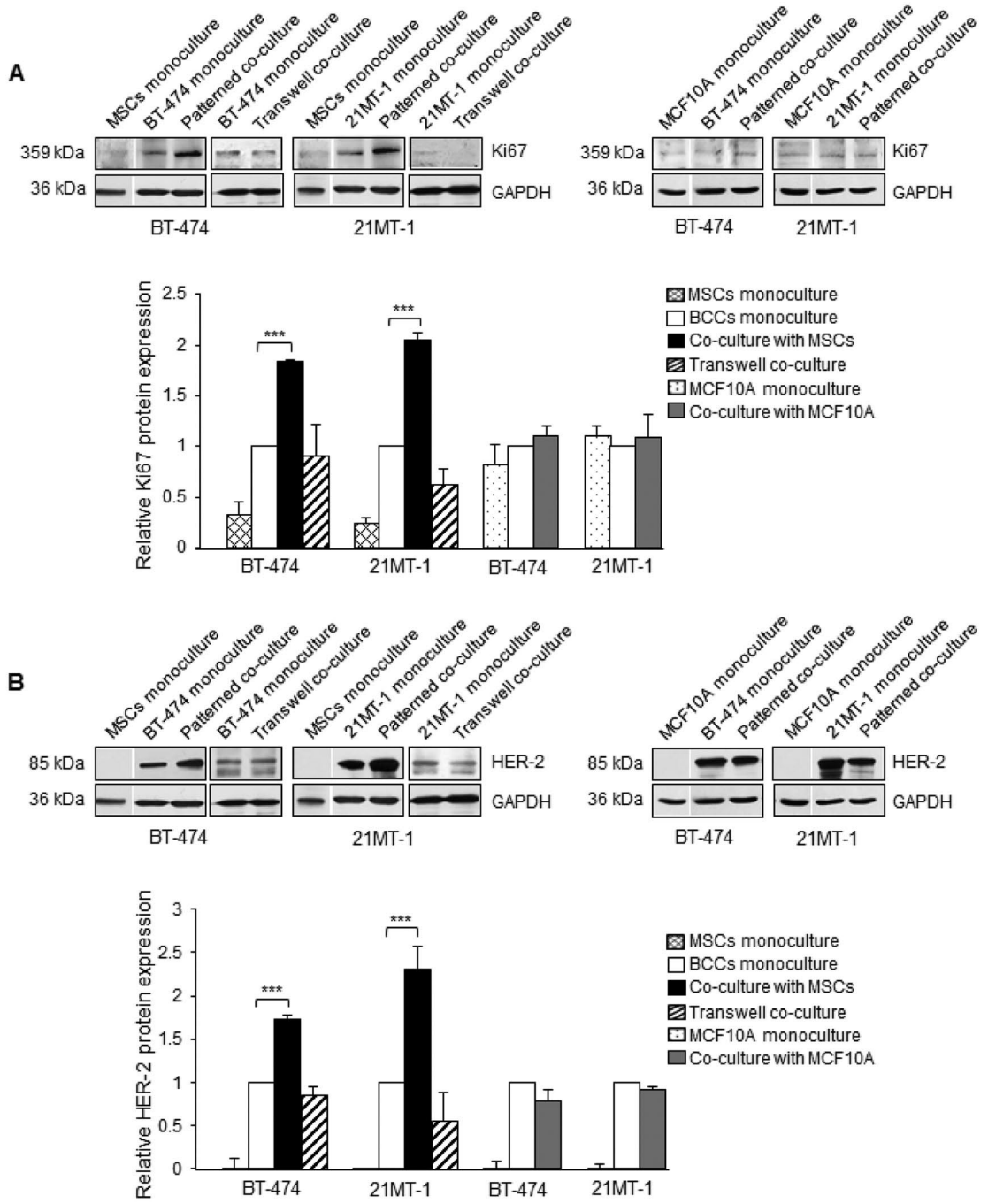

Figure 5. Coculture emulates tumor progression.

(**A**) Upper panel shows representative immunoblot image of protein expression of Ki67 in BT-474 and 21MT-1 breast cancer cells (BCCs) cocultured with MSCs and MCF10A cells. Lower panel shows densitometry analysis of bands normalized with respective BCCs monocultures. ***$p < 0.001$ vs BCCs monoculture.

(**B**) Upper panel shows representative immunoblot image of protein expression of HER-2 in BT-474 and 21MT-1 breast cancer cells cocultured with MSCs and MCF10A cells. Lower panel shows densitometry analysis of bands normalized with respective BCCs monocultures. ***$p < 0.001$ vs BCCs monoculture.

sion to model IMC). We also used two different types of stromal cells, mammary epithelial cells (MCF10A) and mesenchymal stem cells (MSCs), to demonstrate the versatility of our platform. Since MCF10A are nontumorigenic cells and MSCs have a significant role in metastasis, our platform provides an opportunity to study cell−cell interactions in a heterogeneous TME, an inimitable property of cancer progression. The preferential attachment of breast cancer cells to SPS surfaces enabled the use of this system as a template for patterned cocultures with stromal cells on synthetic PEM surfaces. To distinguish two cell populations in patterned coculture system, breast cancer cells were stained with CFDSE dye (green) and stromal cells were stained with PKH26 dye (red). Fluorescence images of breast cancer cells and stromal cells showed distinct patterns of breast cancer cells on day 4 in coculture (Figure 4). We examined the reusability of these patterns. The cells were removed from the patterns with trypsin-EDTA and washed with PBS to ensure that the cells were completely removed from the patterned surfaces. A fresh batch of breast cancer cells was subsequently seeded onto the reused patterns and resulted in the formation of the patterns again (data not shown).

3.4. Coculture Emulates Tumor Progression. To further validate our model at functional level, we investigated the changes in key clinical markers prominently used for tumor diagnosis, in-

cluding tumor and proliferation in our coculture platform (Figure 5). Western blot analysis was performed on the coculture of breast cancer cells BT-474 and 21MT-1 with MSC and MCF10A to study tumor progression and proliferative rates using HER2 and Ki67 as respective markers with mono culture of breast cancer cells and MSCs as controls. Previously, MSCs have been demonstrated to induce increase proliferation and tumor growth of breast tumor.[8−10] Since, MCF10A are normal mammary epithelial cells, no change in proliferation is anticipated. Our data showed a significant upregulation of Ki67 protein expression in cocultures of breast cancer cells with MSCs, while no significant change was observed in cells in transwell coculture, and monocultures of breast cancer cells and MSCs indicating that the direct cell−cell contact is key to this phenomenon (Figure 5A). Furthermore, no significant increase in Ki67 expression was observed in breast cancer cells in coculture with MCF10A cells, suggesting the role of MSCs in tumor progression. Furthermore, a significant upregulation of HER-2 protein expression was observed in cocultures of breast cancer cells with MSCs (Figure 5B) but not in transwell cocultures of breast cancer cells/MSCs and cocultures of breast cancer cells/MCF10A. Such changes are indicative of a net increase in cell growth (vs. apoptosis) and development of an aggressive tumor that would be consistent with the morphologic transition in both the IDC and IMC stages. In the comparison between BT474/MSCs coculture (IDC-like) and 21MT1/MSCs coculture (IMC-like), HER-2 expression was significantly higher in the IMC model. These results demonstrate that the breast cancer cells in the IMC model indicated increase in tumor malignancy, which is similar to the transition observed in the clinical testing of IDC and IMC tumor samples.[46−52]

3.5. Coculture Emulates miRNA Profiles of Clinical Conditions. Microarray analysis on BT474/MSC and 21MT1/MSC coculture models showed that several miRNAs, including miRNA-21 and miRNA-34a, were regulated (data not shown). Clinical studies have shown that miRNA-21 is upregulated in all pathways in breast cancer and plays an important role in deregulating many genes leading to the development of breast cancer.[53−55] miRNA-34a, a tumor suppressor miRNA, was reported to have significant influence on cell cycle, proliferation, migration, invasion, and self-renewal in breast cancer cells.[56−58] qRT-PCR on BT474/MSCs coculture and 21MT1/MSCs coculture was performed to validate the microarray data and profile the miRNA expression in the two breast cancer models with monoculture of breast cancer cells and MSCs as controls (Figure 6). The expression levels of miR-21 were increased in both coculture models while the expression levels of miR-34a were decreased in IDC coculture model compared to a monoculture of breast cancer cells. This data is representative of the miRNA expression trend observed in clinical breast tumor tissues. The coculture model mimics breast cancer progression and shows stage-specific miRNA expression patterns.

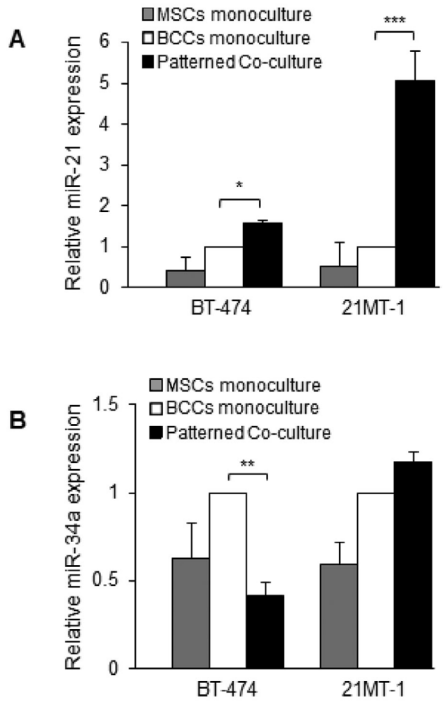

Figure 6. Coculture emulates miRNA profiles of clinical conditions. (**A**) Relative gene expression of miR-21 in BT-474 and 21MT-1 breast cancer cells (BCCs) cocultured with MSCs after normalization with respective BCCs monocultures. *p < 0.05 vs BCCs monoculture; ***p < 0.001 vs BCCs monoculture. (**B**) Relative gene expression of miR- 34a in BT-474 and 21MT-1 breast cancer cells cocultured with MSCs after normalization with respective BCCs monocultures. **p < 0.01 vs BCCs monoculture.

4. Discussion

Breast cancer continues to be a major focus of medical research due to its extensive socioeconomic impact. The majority of the studies directly target tumor cells; however, the clinical success of these studies to develop mechanistic understanding and antitumor therapies remains limited. Recently, cancer cell−stromal cell communications are strongly believed to play a significant role in cancer initiation, progression, and drug responsiveness.[5−7] Here, we report the development of patterned cocultures of breast cancer cells and stromal cells as in vitro models of breast tumors. Our in vitro platform is capable of recreating the dynamics of various stages of breast tumors. Communication between breast cancer cells and stromal cells has been widely recognized to play an important role in cancer initiation, promotion, progression, and development of resistance to treatment.[5−7] Cancer cells maneuver the TME to favor cancer progression and metastasis by influencing stromal cells and the ECM.[59−62] On the other hand, the stromal cells such as MSCs and epithelial cells carry the local tissue architectural cues and influence the cancer behavior.[63−65] Animal experiments have made a significant contribution to understanding human diseases, including breast cancer.[11−14] However, they lack the ability to intercept communication signals and to create snapshots of different tumor stages in order to better predict the effectiveness of treatment strategies in clinical settings. The in situ coculture model developed in this study allows interaction between stromal cells (MSC, MCF10A) and tumor cells in a controlled microenvironment and emulates the temporal progression of the diseases, especially the evolution of genetic morphosis. The significant advantages of our platform are (1) the protein-free cell-culture environment reduces nonspecific function; (2) the physical contact between stromal cells and cancer cells established in our platform facilitates to investigate the role of direct cell−cell interaction in tumor biology; and (3) the cancer−stromal cell interaction can be controlled by pattern dimensions to emulate different stages of a breast tumor. This platform further demon-

strates the capability of our in vitro coculture model to recapitulate the trends observed in clinically relevant biomarkers (HER-2 and Ki67 expression).[46−52] We also demonstrate that our coculture platform mimics the miRNA- 21 and miRNA-34a expression observed in clinical breast tumor samples.[56−58,66−68] To our knowledge, no study has specifically investigated and demonstrated the role of stromal cells in regulation of miRNA expression in breast cancer. Our in vitro platform replicates the clinically observed trend with markers implicated to tumor stages and biology.

The advent of new approaches and diagnostic tests has led to validating Ki67 and HER-2 as important prognostic and predictive markers. Ki67 is a nuclear nonhistone protein, and an antigen associated with cell proliferation and a strong correlation has been found between the percentage of cells positive for Ki67 and nuclear grade, age, and mitotic rate in breast cancer.[46,47] Cheang and co-workers demonstrated that immunopanel of HER2 and Ki67 can segregate the luminal A and B subtypes of breast cancers.[48] This clinical study indicated that a differential Ki67 expression was suitable to discriminate between the subtypes with higher expression classified as luminal B breast cancers having worse prognosis for both breast cancer recurrence and survival while lower expression classified as luminal A tumors. Numerous studies have shown that breast cancers overexpressing Ki67 in more than 20%−50% of the cells are at high risk of developing recurrent disease, showing a statistically significant correlation with clinical outcome, such as disease-free survival or overall survival.[46−49] HER2 plays an important role in promoting oncogenic transformation and tumor growth.[50−52] 25%−30% of the breast cancer patients overexpress HER2 protein, and this overexpression is correlated with a poor clinical outcome.[50−52] Clinical studies have demonstrated that tumors with HER2 protein and gene overexpression showed a high concordance between the primary tumors and their metastases (97%).[69] Majority of these studies have been performed in clinical patient tissues and animal models, however these are time-consuming and complicated to use the data for identifying the subtypes of the cancer. Our in vitro platform mimicked the clinical observations when the tumor cells were in direct contact with MSCs, where in the Ki67 and HER-2 protein expression was significantly ($p < 0.001$) higher compared to the tumor cells alone. Furthermore, this effect was not observed when the tumor cells were in direct contact with MCF10A cells. This demonstrates that our in vitro models can better represent the human tumors to investigate the underlying mechanisms of tumor progression between different subtypes and understand the role of stromal cells in the dynamic and heterogeneous behavior of cancers that mediates tumor progression and influences treatment response and outcomes. Our platform also paves way to Precision Medicine focusing on understanding complex interactions that are encountered but hard to dissect in clinical human samples while minimizing analysis times.

Recent studies indicate that microRNA (miRNA) is an effective biomarker for a variety of diseases, including breast cancer.[53−58] MiRNA are a new class of RNAs that are involved in regulating mRNA expression at the post-transcriptional level and have an active role in gene regulation.[70,71] Several of them are uniquely produced in cancer cells where they upregulate (or downregulate) the synthesis of certain proteins, leading to the formation of tumors. Microarray-based profiling of tumor samples from breast cancer patients found that miRNA-21 was consistently upregulated in several types of breast cancer, suggesting a role for this miRNA in mammary tumor initiation or progression.[66] Additionally, miRNA-21 has also been identified as a marker for breast cancer and predictor of stage with higher expression at later stages of breast cancer.[53−55] We demonstrated that miRNA-21 expression is upregulated in both breast cancer cells cocultured with MSCs. Interestingly, we observed miRNA-21 expression was significantly higher in the 21MT1/MSCs coculture (IMC-like) compared to BT474/MSCs coculture (IDC-like). miRNA-21 has been found to be significantly higher in breast tumors with high proliferation index, advanced tumor staging, node involvement, and aggressive phenotype.[53−55] Our coculture demonstrates a similar phenotype wherein we observe significantly higher Ki67 expression in both IMC-like and IDC-like models which is indicative of high proliferation index. Huang and co-workers showed that the miRNA-21 expression is correlated with HER- 2 upregulation and identified that miRNA-21 induces HER2- induced cancer cell invasion and miRNA-21 overexpression is a key phenotype in HER-2-positive breast cancer patients.[72] These clinical results were emulated in our in vitro platform where we showed that the HER-2 expression is significantly upregulated in the coculture model which is indicative of advanced tumor staging and aggressive phenotype similar to the transition observed in the clinical testing of IDC and IMC tumor samples.[56−58,66−68] MiRNA-34a is a potent tumor suppressor and abrogation of miRNA-34a function could contribute to aberrant cell proliferation, leading to cancer development.[56−58] Kato and co-workers demonstrated that low expression of miRNA-34a has been found in breast cancer cells.[73] Roth and co-workers showed that circulating levels of miRNA-34a correlate with the presence of overt metastases in breast cancer patients.[74] Peurala et al. have shown that miRNA-34a acts as a tumor suppressor and when expressed exerts an independent effect for a lower risk of recurrence or death in breast cancer.[75] This study observed low expression of miRNA-34a in about 32% and high expression in about 25% of the tumors. High miRNA-34a expression was correlated with an aggressive phenotype of breast tumors with high tumor grade and high proliferation rate of the tumors (IMC-like) while low expression of miRNA-34a was correlated with early stages of breast cancer (IDC-like). This indicates that miRNA-34a profile signature varies with the stage of the breast cancer and this also might explain the discrepant data on the miRNA- 34a expression in diverse tumor entities that have been described. miRNA-34a has been reported to be downregulated in nonsmall cell lung carcinomas, pancreas tumor cell lines, colon carcinomas and primary neuroblastomas.[76,77] In contrast, Dutta and co-workers observed a high incidence of miRNA-34a overexpression in various tumor types.[78] Consistent with the data of Peurala et al.,[75] we detected varying miRNA-34a levels in our coculture platform depending on the source of the cells. BT474/MSCs coculture (IDC-like) had a significant downregulation of miRNA-34a expression while 21MT1/MSCs coculture (IMC-like) had a slight upregulation of miRNA-34a expression, thus indicative of the emulation of the corresponding tumor stages observed in clinical samples.

In summary, we demonstrated an innovative approach to engineer coculture of breast cancer and stromal cells, using the polyelectrolyte multilayers (PEM films) and capillary force lithography (CFL). This approach has several advantages over the method used by other groups. The advantages include its high

fidelity, ease of duplication, ability to provide topographical features, ability to print a variety of molecules with nanometer resolution and without the need for dust-free environments and harsh chemical treatments. We have provided evidence that our platform emulates the different stages of the breast tumor by modeling IDC-like and IMC-like systems. To validate the mimicry of the clinical conditions, we demonstrated that the proliferative index (Ki67 expression) and tumor aggressiveness (HER-2 expression) in our coculture platform is similar to the clinical samples. Furthermore, we also demonstrated that our model provides the ability to capture the temporal change in the miRNA signature as the breast tumor develops through various stages. The key advantage of our coculture in situ breast tumor model is the ability to tailor the transitions between different stages of breast cancer by recreating and controlling the cell−cell interactions in play as the breast tumor progresses. This platform provides a robust system to compare the temporal changes in miRNA expression to segregate the cancer subtypes. In the future, this platform will provide an important tool for unlocking some of the intricacies of the miRNA-mediated molecular influences on early breast progression and potentially target specific processes to effectively stop breast cancer progression. The engineered coculture platform also lays groundwork toward precision medicine where in patient-derived tumor cells can be incorporated within our in vitro models to identify potential pathways and drug treatment regimens for individual patients.

Supporting Information is included following the **References**.

Author Contributions — S.K. and A.D. designed and managed the research work; A.D. and K.M.B. performed the experiments; S.K. and A.D. wrote and revised the manuscript.

Acknowledgments — This work was supported by start-up funds from UNL, Layman's Award, NSF-MRSEC Seed Grant, UNL Interdisciplinary Award, and funds from the University of Nebraska UCARE program. The authors would also like to thank Dr. Hamid Band and Dr. Vimla Band (University of Nebraska Medical Center, Omaha, NE) for kindly providing BT-474 and SKBr3 breast cancer cells. The authors also thank Olivia Scheideler for help with the graphics and generation of CFL figures. The authors declare no competing financial interest.

References

(1) Rosenberg, P.S.; Barker, K. A.; William, F.; Anderson. Abstract 3699: Estrogen receptor status and the future burden of invasive and in-situ breast cancers in the United States. *Cancer Res.* 2015, *75*, 3699.

(2) Jiang, P.; Li, X.; Thompson, C. B.; Huang, Z.; Araiza, F.; Osgood, R.; Wei, G.; Feldmann, M.; Frost, G. I.; Shepard, H. M. Effective targeting of the tumor microenvironment for cancer therapy. *Anticancer Res.* 2012, *32* (4), 1203−12.

(3) Cichon, M. A.; Degnim, A. C.; Visscher, D. W.; Radisky, D. C. Microenvironmental influences that drive progression from benign breast disease to invasive breast cancer. *Journal of mammary gland biology and neoplasia* 2010, *15* (4), 389−97.

(4) Bissell, M. J.; Hines, W. C. Why don't we get more cancer? A proposed role of the microenvironment in restraining cancer progression. *Nat. Med.* 2011, *17* (3), 320−9.

(5) Roodhart, J. M.; Daenen, L. G.; Stigter, E. C.; Prins, H. J.; Gerrits, J.; Houthuijzen, J. M.; Gerritsen, M. G.; Schipper, H. S.; Backer, M. J.; van Amersfoort, M.; Vermaat, J. S.; Moerer, P.; Ishihara, K.; Kalkhoven, E.; Beijnen, J. H.; Derksen, P. W.; Medema, R. H.; Martens, A. C.; Brenkman, A. B.; Voest, E. E. Mesenchymal stem cells induce resistance to chemotherapy through the release of platinum-induced fatty acids. *Cancer Cell* 2011, *20* (3), 370−83.

(6) Li, H. J.; Reinhardt, F.; Herschman, H. R.; Weinberg, R. A. Cancer-stimulated mesenchymal stem cells create a carcinoma stem cell niche via prostaglandin E2 signaling. *Cancer Discovery* 2012, *2* (9), 840−55.

(7) Karnoub, A. E.; Dash, A. B.; Vo, A. P.; Sullivan, A.; Brooks, M. W.; Bell, G. W.; Richardson, A. L.; Polyak, K.; Tubo, R.; Weinberg, R. A. Mesenchymal stem cells within tumour stroma promote breast cancer metastasis. *Nature* 2007, *449* (7162), 557−63.

(8) Beckermann, B. M.; Kallifatidis, G.; Groth, A.; Frommhold, D.; Apel, A.; Mattern, J.; Salnikov, A. V.; Moldenhauer, G.; Wagner, W.; Diehlmann, A.; Saffrich, R.; Schubert, M.; Ho, A. D.; Giese, N.; Buchler, M. W.; Friess, H.; Buchler, P.; Herr, I. VEGF expression by mesenchymal stem cells contributes to angiogenesis in pancreatic carcinoma. *Br. J. Cancer* 2008, *99* (4), 622−31.

(9) Bergfeld, S. A.; DeClerck, Y. A. Bone marrow-derived mesenchymal stem cells and the tumor microenvironment. *Cancer Metastasis Rev.* 2010, *29* (2), 249−61.

(10) Zhou, C.; Zhong, Q.; Rhodes, L. V.; Townley, I.; Bratton, M. R.; Zhang, Q.; Martin, E. C.; Elliott, S.; Collins-Burow, B. M.; Burow, M. E.; Wang, G. Proteomic analysis of acquired tamoxifen resistance in MCF-7 cells reveals expression signatures associated with enhanced migration. *Breast cancer research: BCR* 2012, *14* (2), R45.

(11) Borowsky, A. D. Choosing a mouse model: Experimental biology in context—The utility and limitations of mouse models of breast cancer. *Cold Spring Harbor Perspect. Biol.* 2011, *3* (9), a009670.

(12) Vargo-Gogola, T.; Rosen, J. M. Modelling breast cancer: One size does not fit all. *Nat. Rev. Cancer* 2007, *7* (9), 659−72.

(13) Cardiff, R. D.; Moghanaki, D.; Jensen, R. A. Genetically engineered mouse models of mammary intraepithelial neoplasia. *Journal of mammary gland biology and neoplasia* 2000, *5* (4), 421−37.

(14) Medina, D. The preneoplastic phenotype in murine mammary tumorigenesis. *Journal of mammary gland biology and neoplasia* 2000, *5* (4), 393−407.

(15) Chan, C. T.; Qi, J.; Smith, W.; Paranol, R.; Mazitschek, R.; West, N.; Reeves, R.; Chiosis, G.; Schreiber, S. L.; Bradner, J. E.; Paulmurugan, R.; Gambhir, S. S. Syntheses and discovery of a novel class of cinnamic hydroxamates as histone deacetylase inhibitors by multimodality molecular imaging in living subjects. *Cancer Res.* 2014, *74* (24), 7475−86.

(16) Richmond, A.; Su, Y. Mouse xenograft models vs GEM models for human cancer therapeutics. *Dis. Models & Mech.* 2008, *1* (2−3), 78−82.

(17) Benam, K. H.; Dauth, S.; Hassell, B.; Herland, A.; Jain, A.; Jang, K. J.; Karalis, K.; Kim, H. J.; MacQueen, L.; Mahmoodian, R.; Musah, S.; Torisawa, Y. S.; van der Meer, A. D.; Villenave, R.; Yadid, M.; Parker, K. K.; Ingber, D. E. Engineered in vitro disease models. *Annu. Rev. Pathol.: Mech. Dis.* 2015, *10*, 195−262.

(18) Ingber, D. E. Can cancer be reversed by engineering the tumor microenvironment? *Semin. Cancer Biol.* 2008, *18* (5), 356−64.

(19) Weigelt, B.; Ghajar, C. M.; Bissell, M. J. The need for complex 3D culture models to unravel novel pathways and identify accurate biomarkers in breast cancer. *Adv. Drug Delivery Rev.* 2014, *69−70*, 42− 51.

(20) Ghajar, C. M.; Bissell, M. J. Tumor engineering: The other face of tissue engineering. *Tissue Eng., Part A* 2010, *16* (7), 2153−6.

(21) DelNero, P.; Song, Y. H.; Fischbach, C. Microengineered tumor models: Insights & opportunities from a physical sciences-oncology perspective. *Biomed. Microdevices* 2013, *15* (4), 583−93.

(22) Miki, Y.; Ono, K.; Hata, S.; Suzuki, T.; Kumamoto, H.; Sasano, H. The advantages of co-culture over mono cell culture in simulating in vivo environment. *J. Steroid Biochem. Mol. Biol.* 2012, *131* (3−5), 68−75.

(23) Guldner, I. H.; Zhang, S. A journey to uncharted territory: New technical frontiers in studying tumor-stromal cell interactions. *Integrative biology: Quantitative biosciences from nano to macro* 2015, *7* (2), 153−61.

(24) Kidambi, S.; Lee, I.; Chan, C. Primary Neuron/Astrocyte Co-Culture on Polyelectrolyte Multilayer Films: A Template for Studying Astrocyte-Mediated Oxidative Stress in Neurons. *Adv. Funct. Mater.* 2008, *18* (2), 294−301.

(25) Kidambi, S.; Sheng, L.; Yarmush, M. L.; Toner, M.; Lee, I.; Chan, C. Patterned co-culture of primary hepatocytes and fibroblasts using polyelectrolyte multilayer templates. *Macromol. Biosci.* 2007, *7* (3), 344−53.

(26) Khademhosseini, A.; Ferreira, L.; Blumling, J., 3rd; Yeh, J.; Karp, J. M.; Fukuda, J.; Langer, R. Co-culture of human embryonic stem cells with murine embryonic fibroblasts on microwell-patterned substrates. *Biomaterials* 2006, *27* (36), 5968−77.

(27) Fukuda, J.; Khademhosseini, A.; Yeh, J.; Eng, G.; Cheng, J.; Farokhzad, O. C.; Langer, R. Micropatterned cell co-cultures using layer-by-layer deposition of extracellular matrix components. *Biomaterials* 2006, *27* (8), 1479−86.

(28) Co, C. C.; Wang, Y.-C.; Ho, C.-C. Biocompatible Micropatterning of Two Different Cell Types. *J. Am. Chem. Soc.* 2005, *127* (6), 1598−1599.

(29) Mendelsohn, J. D.; Yang, S. Y.; Hiller, J.; Hochbaum, A. I.; Rubner, M. F. Rational design of cytophilic and cytophobic polyelectrolyte multilayer thin films. *Biomacromolecules* 2003, *4* (1), 96−106.

(30) Decher, G. Fuzzy nanoassemblies: toward layered polymeric multicomposites. *Science* 1997, *277* (5330), 1232−1237.

(31) Vodouhe, C.; Schmittbuhl, M.; Boulmedais, F.; Bagnard, D.; Vautier, D.; Schaaf, P.; Egles, C.; Voegel, J. C.; Ogier, J. Effect of functionalization of multilayered polyelectrolyte films on motoneuron growth. *Biomaterials* 2005, *26* (5), 545−554.

(32) Boura, C.; Muller, S.; Vautier, D.; Dumas, D.; Schaaf, P.; Voegel, J. C.; Stoltz, J. F.; Menu, P. Endothelial cell-interactions with polyelectrolyte multilayer films. *Biomaterials* 2005, *26* (22), 4568− 4575.

(33) Kidambi, S.; Udpa, N.; Schroeder, S. A.; Findlan, R.; Lee, I.; Chan, C. Cell Adhesion on Polyelectrolyte Multilayer Coated Polydimethylsiloxane Surfaces with Varying Topographies. *Tissue Eng.* 2007, *13*, 2105.

(34) Hong, J.; Alvarez, L. M.; Shah, N. J.; Griffith, L. G.; Kim, B. S.; Char, K.; Hammond, P. T. Multilayer thin film coatings capable of extended programmable drug release: application to human mesenchymal stem cell differentiation. *Drug Delivery Transl. Res.* 2012, *2* (5), 375−83.

(35) Arias, C. J.; Keller, T. C., 3rd; Schlenoff, J. B. Quasi-Spherical Cell Clusters Induced by a Polyelectrolyte Multilayer. *Langmuir* 2015, *31* (23), 6436−46.

(36) Pattabhi, S. R.; Lehaf, A. M.; Schlenoff, J. B.; Keller, T. C., 3rd Human mesenchymal stem cell osteoblast differentiation, ECM deposition, and biomineralization on PAH/PAA polyelectrolyte multilayers. *J. Biomed. Mater. Res., Part A* 2015, *103* (5), 1818−27.

(37) Martinez, J. S.; Lehaf, A. M.; Schlenoff, J. B.; Keller, T. C., 3rd Cell durotaxis on polyelectrolyte multilayers with photogenerated gradients of modulus. *Biomacromolecules* 2013, *14* (5), 1311−20.

(38) Berg, M. C.; Yang, S. Y.; Hammond, P. T.; Rubner, M. F. Controlling mammalian cell interactions on patterned polyelectrolyte multilayer surfaces. *Langmuir* 2004, *20* (4), 1362−8.

(39) Kidambi, S.; Lee, I.; Chan, C. Controlling primary hepatocyte adhesion and spreading on protein-free polyelectrolyte multilayer films. *J. Am. Chem. Soc.* 2004, *126* (50), 16286−16287.

(40) Li, M. Y.; Kondabatni, K. K.; Cui, T. H.; McShane, M. J. Fabrication of 3-D gelatin-patterned glass substrates with layer-by-layer and lift-off (LbL-LO) technology. *IEEE Trans. Nanotechnol.* 2004, *3* (1), 115−123.

(41) Shaikh Mohammed, J.; DeCoster, M. A.; McShane, M. J. Micropatterning of nanoengineered surfaces to study neuronal cell attachment in vitro. *Biomacromolecules* 2004, *5* (5), 1745−1755.

(42) Daverey, A.; Mytty, A. C.; Kidambi, S. Topography Mediated Regulation of Her-2 Expression in Breast Cancer Cells. *Nano LIFE* 2012, *2* (3), 1241009.

(43) Clark, S. L.; Montague, M. F.; Hammond, P. T. Ionic Effects of Sodium Chloride on the Templated Deposition of Polyelectrolytes Using Layer-by-Layer Ionic Assembly. *Macromolecules* 1997, *30*, 7237−7244.

(44) Mendelsohn, J. D.; Yang, S. Y.; Hiller, J. A.; Hochbaum, A. I.; Rubner, M. F. Rational Design of Cytophilic and Cytophobic Polyelectrolyte Multilayer Thin Films. *Biomacromolecules* 2003, *4* (1), 96−106.

(45) Farhat, T. R.; Schlenoff, J. B. Doping-controlled ion diffusion in polyelectrolyte multilayers: Mass transport in reluctant exchangers. *J. Am. Chem. Soc.* 2003, *125* (15), 4627−36.

(46) Sahin, A. A.; Ro, J.; Ro, J. Y.; Blick, M. B.; el-Naggar, A. K.; Ordonez, N. G.; Fritsche, H. A.; Smith, T. L.; Hortobagyi, G. N.; Ayala, A. G. Ki-67 immunostaining in node-negative stage I/II breast carcinoma. Significant correlation with prognosis. *Cancer* 1991, *68* (3), 549−57.

(47) Keshgegian, A. A.; Cnaan, A. Proliferation markers in breast carcinoma. Mitotic figure count, S-phase fraction, proliferating cell nuclear antigen, Ki-67 and MIB-1. *Am. J. Clin. Pathol.* 1995, *104* (1), 42−9.

(48) Cheang, M. C.; Chia, S. K.; Voduc, D.; Gao, D.; Leung, S.; Snider, J.; Watson, M.; Davies, S.; Bernard, P. S.; Parker, J. S.; Perou, C. M.; Ellis, M. J.; Nielsen, T. O. Ki67 index, HER2 status, and prognosis of patients with luminal B breast cancer. *Journal of the National Cancer Institute* 2009, *101* (10), 736−50.

(49) Assersohn, L.; Salter, J.; Powles, T. J.; A'Hern, R.; Makris, A.; Gregory, R. K.; Chang, J.; Dowsett, M. Studies of the potential utility of Ki67 as a predictive molecular marker of clinical response in primary breast cancer. *Breast Cancer Res. Treat.* 2003, *82* (2), 113−23.

(50) Slamon, D. J.; Clark, G. M.; Wong, S. G.; Levin, W. J.; Ullrich, A.; McGuire, W. L. Human breast cancer: Correlation of relapse and survival with amplification of the HER-2/neu oncogene. *Science* 1987, *235* (4785), 177−82.

(51) Gusterson, B. A.; Gelber, R. D.; Goldhirsch, A.; Price, K. N.; Save-Soderborgh, J.; Anbazhagan, R.; Styles, J.; Rudenstam, C. M.; Golouh, R.; Reed, R.; et al. Prognostic importance of c-erbB-2 expression in breast cancer. International (Ludwig) Breast Cancer Study Group. *J. Clin. Oncol.* 1992, *10* (7), 1049−56.

(52) Ross, J. S.; Fletcher, J. A. HER-2/neu (c-erb-B2) gene and protein in breast cancer. *Am. J. Clin. Pathol.* 1999, *112* (1 Suppl1), S53−67.

(53) Kumar, S.; Keerthana, R.; Pazhanimuthu, A.; Perumal, P. Overexpression of circulating miRNA-21 and miRNA-146a in plasma samples of breast cancer patients. *Indian J. Biochem. Biophys.* 2013, *50* (3), 210−4.

(54) Li, J.; Zhang, Y.; Zhang, W.; Jia, S.; Tian, R.; Kang, Y.; Ma, Y.; Li, D. Genetic Heterogeneity of Breast Cancer Metastasis May Be Related to miR-21 Regulation of TIMP-3 in Translation. *Int. J. Surg. Oncol.* 2013, *2013*, 875078.

(55) Mar-Aguilar, F.; Luna-Aguirre, C. M.; Moreno-Rocha, J. C.; Araiza-Chavez, J.; Trevino, V.; Rodriguez-Padilla, C.; Resendez-Perez, D. Differential expression of miR-21, miR-125b and miR-191 in breast cancer tissue. *Asia-Pacific Journal of Clinical Oncology* 2013, *9* (1), 53−9.

(56) Li, L.; Yuan, L.; Luo, J.; Gao, J.; Guo, J.; Xie, X. MiR-34a inhibits proliferation and migration of breast cancer through down-regulation of Bcl-2 and SIRT1. *Clin. Exp. Med.* 2013, *13* (2), 109−17.

(57) Hui, C.; Yujie, F.; Lijia, Y.; Long, Y.; Hongxia, X.; Yong, Z.; Jundong, Z.; Qianyong, Z.; Mantian, M. MicroRNA-34a and microRNA-21 play roles in the chemopreventive effects of 3,6-dihydroxyflavone on 1-methyl-1-nitrosourea-induced breast carcinogenesis. *Breast Cancer Research: BCR* 2012, *14* (3), R80.

(58) Kastl, L.; Brown, I.; Schofield, A. C. miRNA-34a is associated with docetaxel resistance in human breast cancer cells. *Breast Cancer Res. Treat.* 2012, *131* (2), 445−54.

(59) Boudreau, A.; van't Veer, L. J.; Bissell, M. J. An "elite hacker": Breast tumors exploit the normal microenvironment program to instruct their progression and biological diversity. *Cell Adhes. Migr.* 2012, *6* (3), 236.

(60) Lo, A. T.; Mori, H.; Mott, J.; Bissell, M. J. Constructing Three-Dimensional Models to Study Mammary Gland Branching Morphogenesis and Functional Differentiation. *J. Mammary Gland Biol. Neoplasia* 2012, *17*, 103.

(61) Correia, A. L.; Bissell, M. J. The tumor microenvironment is a dominant force in multidrug resistance. *Drug Resist. Updates* 2012, *15* (1−2), 39−49.

(62) Nistico, P.; Bissell, M. J.; Radisky, D. C. Epithelial-mesenchymal transition: General principles and pathological relevance with special emphasis on the role of matrix metalloproteinases. *Cold Spring Harbor Perspect. Biol.* 2012, *4* (2), a011908.

(63) Shin, S. Y.; Nam, J.-S.; Lim, Y.; Lee, Y. H. TNFα-exposed Bone Marrow-derived Mesenchymal Stem Cells Promote Locomotion of MDA-MB-231 Breast Cancer Cells through Transcriptional Activation of CXCR3 Ligand Chemokines. *J. Biol. Chem.* 2010, *285* (40), 30731− 30740.

(64) Geiger, T. R.; Peeper, D. S. Metastasis mechanisms. *Biochim. Biophys. Acta, Rev. Cancer* 2009, *1796* (2), 293−308.

(65) Spaeth, E. L.; Dembinski, J. L.; Sasser, A. K.; Watson, K.; Klopp, A.; Hall, B.; Andreeff, M.; Marini, F. Mesenchymal stem cell transition to tumor-associated fibroblasts contributes to fibrovascular network expansion and tumor progression. *PLoS One* 2009, *4* (4), e4992.

(66) Iorio, M. V.; Ferracin, M.; Liu, C. G.; Veronese, A.; Spizzo, R.; Sabbioni, S.; Magri, E.; Pedriali, M.; Fabbri, M.; Campiglio, M.; Menard, S.; Palazzo, J. P.; Rosenberg, A.; Musiani, P.; Volinia, S.; Nenci, I.; Calin, G. A.; Querzoli, P.; Negrini, M.; Croce, C. M. MicroRNA gene expression deregulation in human breast cancer. *Cancer Res.* 2005, *65* (16), 7065−70.

(67) Asaga, S.; Kuo, C.; Nguyen, T.; Terpenning, M.; Giuliano, A. E.; Hoon, D. S. Direct serum assay for microRNA-21 concentrations in early and advanced breast cancer. *Clin. Chem.* 2011, *57* (1), 84−91.

(68) Huang, G. L.; Zhang, X. H.; Guo, G. L.; Huang, K. T.; Yang, K. Y.; Shen, X.; You, J.; Hu, X. Q. Clinical significance of miR-21 expression in breast cancer: SYBR-Green I-based real-time RT-PCR study of invasive ductal carcinoma. *Oncol. Rep.* 2009, *21* (3), 673−9.

(69) Joensuu, K.; Leidenius, M.; Kero, M.; Andersson, L. C.; Horwitz, K. B.; Heikkila, P. ER, PR, HER2, Ki-67 and CK5 in Early and Late Relapsing Breast Cancer-Reduced CK5 Expression in Metastases. *Breast Cancer: Basic Clin. Res.* 2013, *7*, 23−34.

(70) Gusev, Y.; Schimdgen, T.; Lerner, M.; Brackett, D. Analysis of microRNA profiling data with systems biology tools. *MicroRNA Profiling in Cancer* 2010, 169−196.

(71) Herschkowitz, J. I.; Fu, X. MicroRNAs add an additional layer to the complexity of cell signaling. *Sci. Signaling* 2011, *4* (184), jc5.

(72) Huang, T. H.; Wu, F.; Loeb, G. B.; Hsu, R.; Heidersbach, A.; Brincat, A.; Horiuchi, D.; Lebbink, R. J.; Mo, Y. Y.; Goga, A.; McManus, M. T. Up-regulation of miR-21 by HER2/neu signaling promotes cell invasion. *J. Biol. Chem.* 2009, *284* (27), 18515−24.

(73) Kato, M.; Paranjape, T.; Ullrich, R.; Nallur, S.; Gillespie, E.; Keane, K.; Esquela-Kerscher, A.; Weidhaas, J. B.; Slack, F. J. The mir-34 microRNA is required for the DNA damage response in vivo in C. elegans and in vitro in human breast cancer cells. *Oncogene* 2009, *28* (25), 2419−24.

(74) Roth, C.; Rack, B.; Muller, V.; Janni, W.; Pantel, K.; Schwarzenbach, H. Circulating microRNAs as blood-based markers for patients with primary and metastatic breast cancer. *Breast Cancer Research: BCR* 2010, *12* (6), R90.

(75) Peurala, H.; Greco, D.; Heikkinen, T.; Kaur, S.; Bartkova, J.; Jamshidi, M.; Aittomaki, K.; Heikkila, P.; Bartek, J.; Blomqvist, C.; Butzow, R.; Nevanlinna, H. MiR-34a expression has an effect for lower risk of metastasis and associates with expression patterns predicting clinical outcome in breast cancer. *PLoS One* 2011, *6* (11), e26122.

(76) Bommer, G. T.; Gerin, I.; Feng, Y.; Kaczorowski, A. J.; Kuick, R.; Love, R. E.; Zhai, Y.; Giordano, T. J.; Qin, Z. S.; Moore, B. B.; MacDougald, O. A.; Cho, K. R.; Fearon, E. R. p53-mediated activation of miRNA34 candidate tumor-suppressor genes. *Curr. Biol.* 2007, *17* (15), 1298−307.

(77) Braun, C. J.; Zhang, X.; Savelyeva, I.; Wolff, S.; Moll, U. M.; Schepeler, T.; Orntoft, T. F.; Andersen, C. L.; Dobbelstein, M. p53- Responsive micrornas 192 and 215 are capable of inducing cell cycle arrest. *Cancer Res.* 2008, *68* (24), 10094−104.

(78) Dutta, K. K.; Zhong, Y.; Liu, Y. T.; Yamada, T.; Akatsuka, S.; Hu, Q.; Yoshihara, M.; Ohara, H.; Takehashi, M.; Shinohara, T.; Masutani, H.; Onuki, J.; Toyokuni, S. Association of microRNA-34a overexpression with proliferation is cell type-dependent. *Cancer Sci.* 2007, *98* (12), 1845−52.

Breast Cancer/Stromal Cells Co-culture on Polyelectrolyte Films Emulates Tumor Stages and miRNA Profiles of Clinical Samples

Amita Daverey[1], Karleen M Brown[1] and Srivatsan Kidambi[1,2,3,*]

[1]Department of Chemical and Biomolecular Engineering,
University of Nebraska-Lincoln, NE, 68588
[2]Nebraska Center for Materials and Nanoscience,
University of Nebraska-Lincoln, NE, 68588
[3]Regenerative Medicine Program,
University of Nebraska Medical Center, NE, 68198.

[*]indicates corresponding author. Email: skidambi2@unl.edu

Supplementary Information

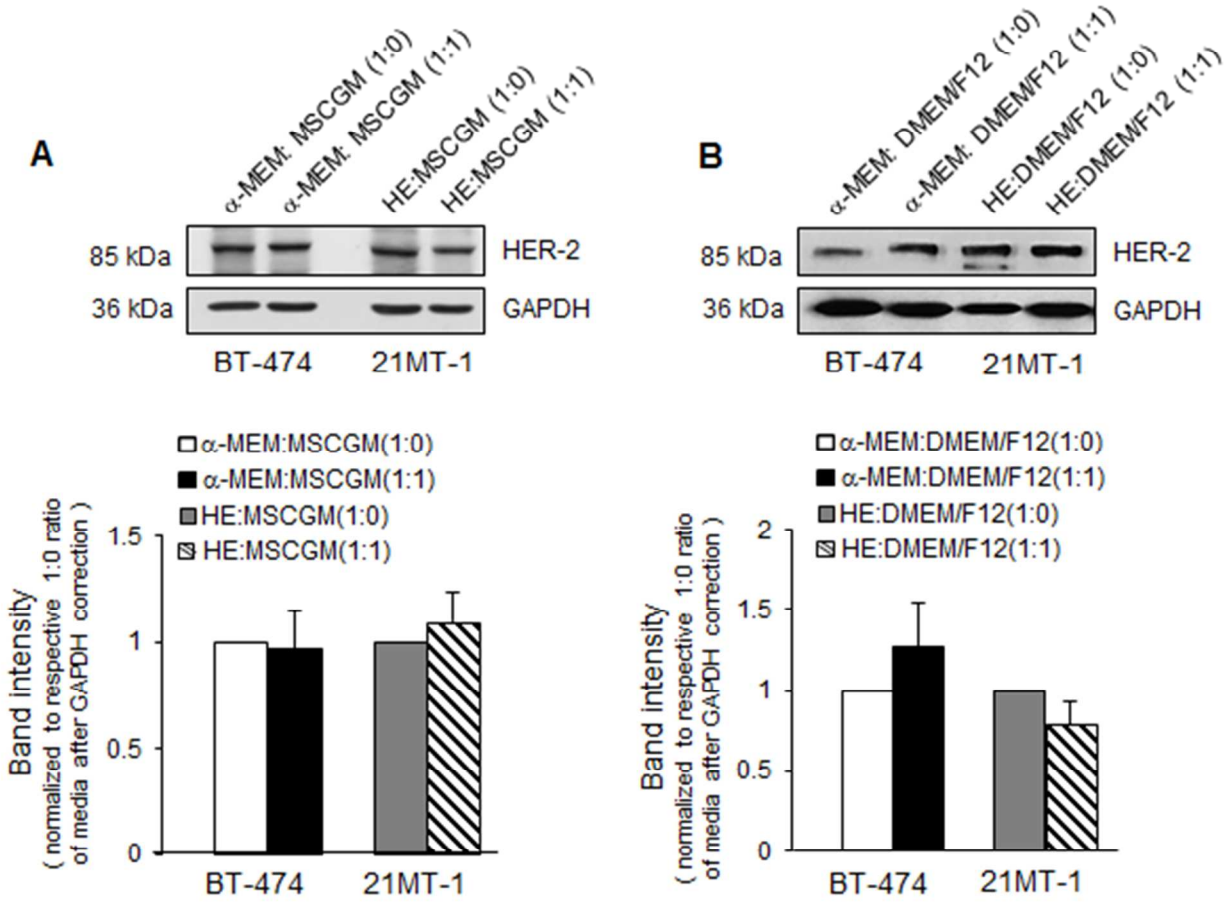

Supplementary Figure 1: ***Optimized culture conditions for the co-culture platform*****.** (A) Upper panel, representative immunoblot shows expression of HER-2 as a marker for breast cancer cell to optimize media condition for co-culture of breast cancer cells with MSCs. Lower panel, densitometry analysis of bands shows no significant change in HER-2 expression when breast cancer cells (MEM/HE) and MSCs (MSCGM) media was used in 1:1 ratio. (B) Upper panel, representative immunoblot shows expression of HER-2 as a marker for breast cancer cell to optimize media condition for co-culture of breast cancer cells with MCF10A. Lower panel, densitometry analysis of bands shows no significant change in HER-2 expression when breast cancer cells (MEM/HE) and MCF10A (DMEM/F12) media was used in 1:1 ratio.